

the TCSC device and its stabilizing signal, respectively. The blocks $F_1(s)$ and $F_2(s)$ relate the TCSC output (variable line susceptance, B_{kj}) with the controlled system variable ($X_{\text{controlled}}$) and the variable used as the input to the stabilizer, X_{inp} . Functions $F_1(s)$ and $F_2(s)$ are of the same order as the number of state variables in the system. The symbol X_{ref} denotes the controller reference, whose value in steady state is close or equal to $X_{\text{controlled}}$.

The TCSC incremental model consists of current injections into the power system network at buses k and j , which are the device terminals. The initial value for its susceptance (B_{kj}^0) is directly modeled into the load flow equations. The incremental susceptance (ΔB_{kj}) is determined, at any instant, by the output of the TCSC controller. The controller dynamics is modeled through a set of differential and algebraic equations.

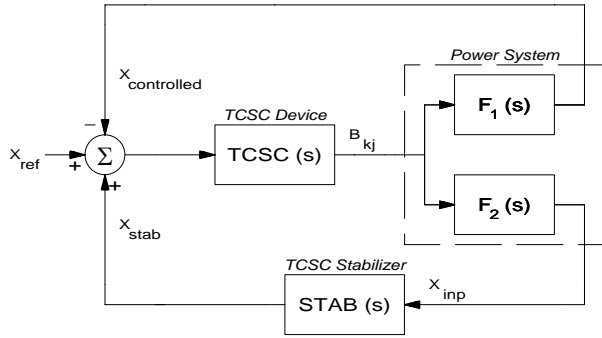


Figure 1. TCSC Control System Diagram

2.2. Background Theory and Proposed Methodology

References [6,10] explain the theoretical aspects concerning the use of transfer function residues to find the most suitable locations for placing damping sources for power system oscillations. Reference [10] uses transfer function residues to find the most suitable generators for placing stabilizers in a large system. Reference [6] uses residues to determine suitable buses, out of all buses in the system, to place the whole static compensator. This differs from the previous generator stabilizer problem in which generator sites are already defined. The use of the *augmented power system equations* [6,7,8,9] is essential to the practical application of these concepts to large scale systems.

The proposed method for siting TCSC devices is an extension of that described for static VAR compensators [6]. The diagram of Figure 2 is used to explain the concepts of this method.

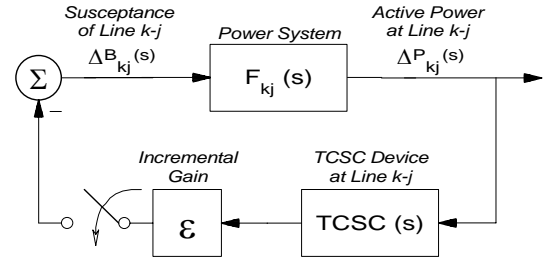


Figure 2. A TCSC of Incremental Gain is Inserted to Line k - j of the Power System

The poles of the open-loop transfer function (OLTF) $F_{kj}(s)$ are the system eigenvalues for the base case studied. The closure of the feedback loop of incremental gain (Figure 2) will cause small deviations in the system eigenvalues [6,10]. These eigenvalue deviations are given by the expression:

$$\Delta \lambda_i = - R_i^{kj} \epsilon \text{ TCSC}(\lambda_i) \quad (1)$$

λ_i being a pole of $F_{kj}(s)$ and R_i^{kj} the associated residue.

A critical (low damped or unstable) eigenvalue λ_c undergoes small changes $\Delta \lambda_c$ which are therefore proportional to the moduli of the residues R_c^{kj} . Note that there exists nl residues R_c^{kj} , where nl is the total number of transmission lines in the system. Transmission line ranking, for placing TCSC devices to damp a critical mode λ_c , can therefore be based on the residues for transfer functions $\Delta P_{kj}(s=\lambda_c) / \Delta B_{kj}(s=\lambda_c)$ of largest moduli, where ΔP_{kj} is the incremental power flow in line between buses k and j and ΔB_{kj} is the change in the susceptance of the same line. Another valuable ranking list can be made from the moduli of the modal controllability factors [6] associated with the input disturbances to line susceptances ΔB_{kj} .

3. TCSC CONTROL ASPECTS ILLUSTRATED ON A LINE POWER SCHEDULING EXERCISE

The small power system of this exercise (see Figure 3 and Appendix) comprises a salient-pole synchronous generator connected to an infinite bus through a double-circuit transmission line. The operating points considered correspond to generation levels of 500 and 1000 MW.

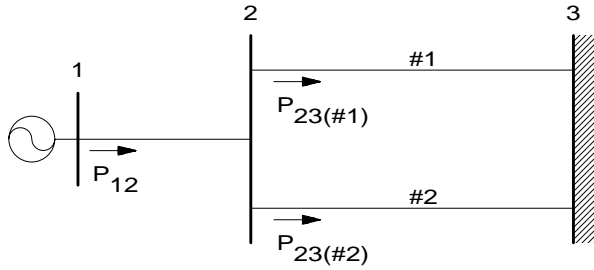


Figure 3. Small Power System

The generator has a 5th order model whose mathematical formulation is fully described in [7]. A first order model of a TCSC device is connected to either line 1-2 or line 2-3(#2) and is considered to be floating (i.e., the impedance between the TCSC terminals is zero) at steady-state.

The block diagram and parameters of the TCSC Proportional-Integral (PI) controller are given in Figure 4. The PI control action is made faster than needed in practice for tutorial purposes.

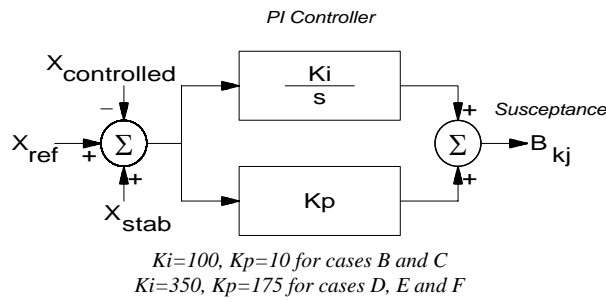


Figure 4. TCSC Controller for All Cases

Two strategies for scheduling the power flow of line 2-3(#2) with a local TCSC device are here implemented simply by changing the $\Delta X_{\text{controlled}}$ signal defined in figures 1 and 4. One strategy maintains the power flow in the line with variable series compensation at a specified value ($\Delta X_{\text{controlled}} = \Delta P_{23(\#2)}$) and will here be referred to as "constant line power" strategy. The opposite strategy is to force the compensated line to absorb all of the increased power dispatch of the line 1-2 ($\Delta X_{\text{controlled}} = \Delta P_{23(\#2)} - \Delta P_{12}$). The latter is known as a "constant-angle" strategy [5] since it keeps the flows on parallel, fixed impedance, paths at constant level.

The "constant angle" control structure proposed in this paper requires the telecommunication of the remote signal ΔP_{12} , but has a reliable and inexpensive practical implementation due to the slow dynamics of the line power scheduling process. In the general case, the increased power interchange to be channeled through a specified transmission corridor is given by the

summation of power flow increments of several lines ($\Sigma \Delta P_{kj}$). The controlled variable for the proposed implementation of the "constant angle" strategy, in the general case, would be $\Delta X_{\text{controlled}} = \Delta P_{tc} - \Sigma \Delta P_{kj}$, where ΔP_{tc} are the power deviations in the specified transmission corridor.

The "constant angle" control strategy can be synthesized with the use of local signals only [5] but it is not as robust to system changes as the simple control structure described in this section.

Table 1 displays the system eigenvalues for different TCSC locations and control strategies. Case A corresponds to the system with no TCSC. Case B includes the action of a TCSC at line 2-3(#2) regulating its own power flow. Case C considers the action of a TCSC at line 1-2 regulating its own power flow. Note that a zero eigenvalue appears indicating an uncontrollable system. The problem has arisen because the TCSC controller imposes a constant power flow at line 1-2 irrespective of angle deviations at its terminals. This problem has not appeared in Case B because line 2-3(#1), which is parallel to the series compensated one, provides a free path for synchronizing power exchanges between the generator and the infinite bus. Case D refers to the system with the TCSC at line 2-3(#2) controlled to absorb all of the increased power flow in line 1-2 ("constant angle" control). This strategy is effected in case D by defining the variable $\Delta X_{\text{controlled}} = \Delta P_{23(\#2)} - \Delta P_{12}$.

A	No TCSC	B	TCSC at line 2-3(#2) "Constant Line Power"
	-24.63		-24.65
	-3.940 ± j6.901		-3.877 ± j6.879
	-6.505		-6.584
	-0.362 ± j6.219		-0.633 ± j5.740
			-2.271
C	TCSC at line 1-2 "Constant Line Power"	D	TCSC at line 2-3(#2) "Constant Angle"
	-27.64		-24.49
	-3.916 ± j6.880		-4.291 ± j6.891
	-6.532		-0.685 ± j8.034
	-0.592 ± j6.027		-7.017
	0.0		-1.652

Table 1. Eigenvalue Results for Cases A, B, C and D (Generation Level of 500 MW)

Step response results of the linearized system are now presented to help evaluating the performance of the different alternatives. The applied disturbance is a 1% step in the mechanical power reference of the synchronous generator. The chosen set of monitored variables are the incremental deviations in active power

flow at the sending end of the three lines of the system (ΔP_{12} , $\Delta P_{23(\#1)}$, $\Delta P_{23(\#2)}$).

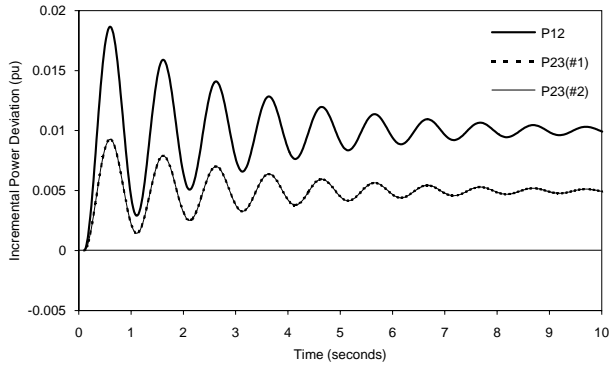


Figure 5. Case A - System with no TCSC Device
($\lambda = -0.362 \pm j6.219$)

Figures 5, 6, 7 and 8 show the system step responses for cases A, B, C, and D, whose eigenvalues were displayed in Table 1. The dominant system eigenvalues are also shown in the captions of these plots. Figure 5 shows that, in the absence of a TCSC device, the power increase ΔP_{12} is equally shared between the two circuits of the transmission line. Case B results (Figure 6) show the power flow in line 2-3(#2) returning to its scheduled pre-disturbance value through TCSC action. The increased power transfer flows solely through the parallel path (line 2-3(#1)).

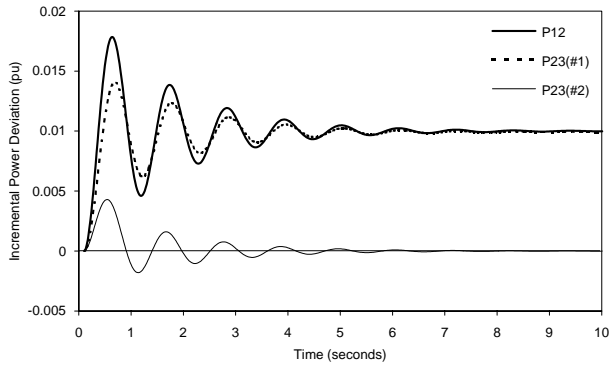


Figure 6. Case B - TCSC at Line 2-3(#2) with
"Constant Line Power" Strategy ($\lambda = -0.633 \pm j5.740$)

Case C results are displayed on an enlarged time scale (Figure 7) to better show system uncontrollability ($\lambda = 0$). The incremental variables plotted in Figure 7 are the voltage angle at bus 2 ($\Delta\theta_2$), in radians, and the active power flows at the sending and receiving ends of line 1-2: $\Delta P_{12}(\text{send})$ and $\Delta P_{12}(\text{rec.})$, both in per unit. The final value of the power increment $\Delta P_{12}(\text{send})$ is equal to the applied step disturbance to the generator mechanical power. The reference to the TCSC controller was left unchanged ($\Delta X_{\text{ref}} = 0$), and therefore a constant error is continuously seen by the

PI controller. The susceptance ΔB_{12} will then raise indefinitely, increasing line current and consequently its resistive losses. Figure 7 shows that active power deviations $\Delta P_{12}(\text{rec.})$ decreases while the bus angle $\Delta\theta_2$ increases.

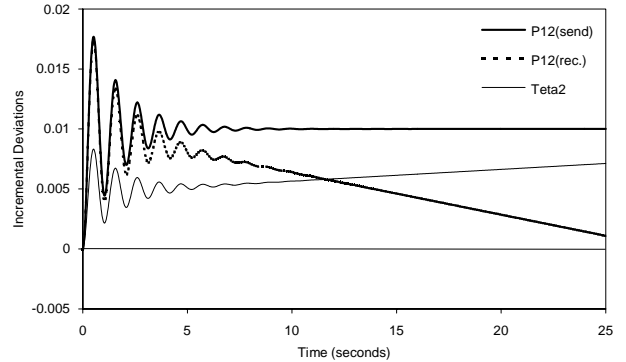


Figure 7. Case C - TCSC at Line 1-2 with
"Constant Line Power" Strategy
($\lambda = -0.592 \pm j6.027$; $\lambda = 0$)

Case D results (Figure 8) show the compensated line 2-3(#2) absorbing all of the increased active power generation. The power flow in the parallel path (line 2-3(#1)) is seen to settle down at the pre-disturbance value.

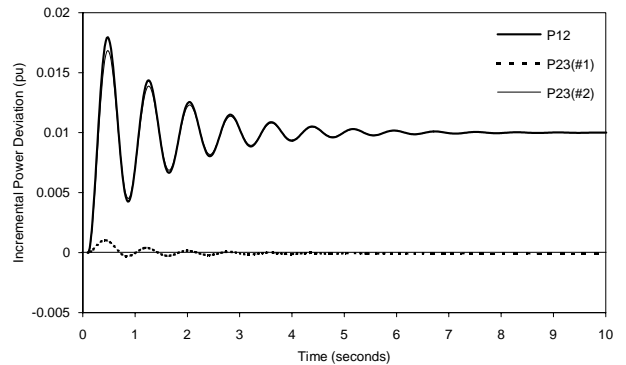


Figure 8. Case D - TCSC at Line 2-3(#2) with
"Constant Angle" Strategy ($\lambda = -0.685 \pm j8.034$)

Consider another system operating point with the generated power raised to 1000 MW. Case E, whose eigenvalues are shown in Table 2, has the same TCSC location and parameters as case D. The electromechanical mode ($\lambda = +0.701 \pm j7.765$) is seen to be highly unstable for case E. A stabilizing signal to the TCSC device can make the system stable for this higher power transfer. Stabilizer design is based on Nyquist plots of a chosen open loop transfer function (OLTF), considering the diagram of Figure 1. Closed loop stability in this case is obtained by a counter-clockwise encirclement of the -1 point by the Nyquist plot of the OLTF after compensation. The reader is referred to

[7,12] for detailed information regarding the frequency response methods of this paper.

Generator speed was chosen as the TCSC stabilizer input ($X_{inp} = \omega_{gen}$) and, therefore, the OLTF of interest is $\Delta\omega_{gen}(s)/\Delta X_{ref}(s)$, where X_{ref} is the TCSC reference. The Nyquist plot of Figure 9 is obtained with the feedback loop of the variable $\Delta X_{controlled}$ closed. Figure 9 directly informs that the feedback controller must provide considerable amplification but minimum phase compensation: only a lag of 11.5° at the center frequency of 7.8 rad/s.

TCSC at line 2-3(#2)	
"Constant Angle" Strategy	
E	No stabilizer
	-23.90
	$-5.348 \pm j6.933$
	-7.820
	$+0.701 \pm j7.765$
	-1.807
F	TCSC with stabilizer
	-23.73
	$-6.416 \pm j6.679$
	$-0.905 \pm j7.741$
	$-6.570 \pm j0.703$
	-1.768
	-0.344

Table 2. Eigenvalues for Cases E and F (Generation Level of 1000 MW)

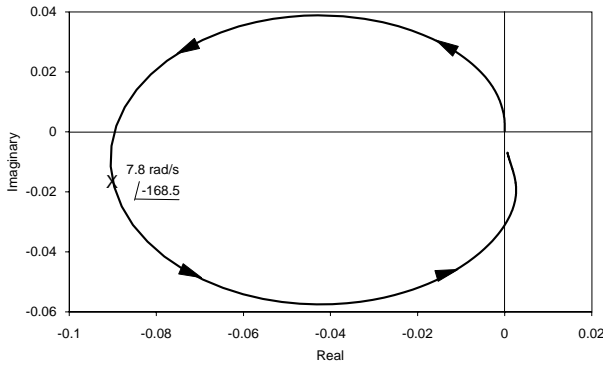


Figure 9. Nyquist Plot of OLTF $\Delta\omega_{gen}(s)/\Delta X_{ref}(s)$ used for TCSC Stabilizer Design ($\lambda = +0.701 \pm j7.765$)

The stabilizer of Figure 10 provides the required compensation and is seen to be very effective from the eigenvalue results of Table 2 (Case F) and the step response plots of Figure 11.

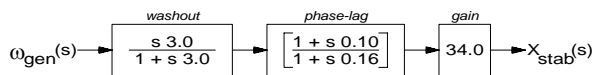


Figure 10. TCSC Stabilizer in Case F

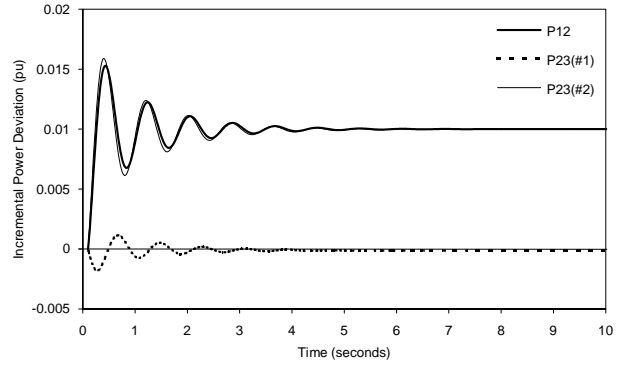


Figure 11. Case F - TCSC at Line 2-3(#2) with "Constant Angle" Strategy and Stabilizer ($\lambda = -0.905 \pm j7.741$)

4. SITING AND TUNING TCSC DEVICES TO DAMP OSCILLATIONS IN A LARGE POWER SYSTEM

The power system analyzed is the 616 bus, 995 line, 50 generator model of the South-Southeast Brazilian System described in [6]. There were stabilizers in 16 generators of the original system model causing all eigenvalues to have damping ratios above 5% for the operating point considered. The system eigenvalues for the same operating point are shown schematically in Figure 12, in the absence of the 16 power system stabilizers.

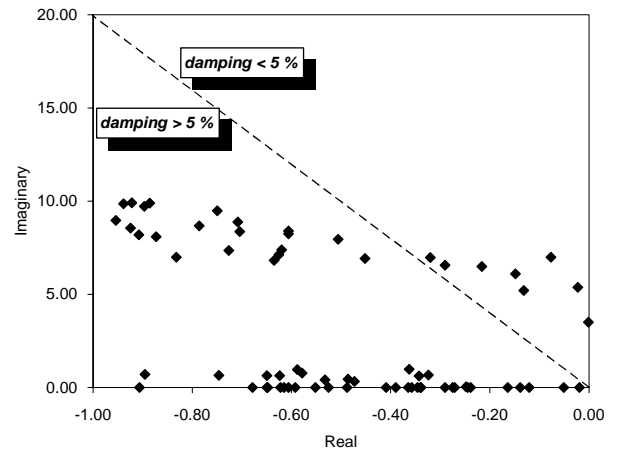


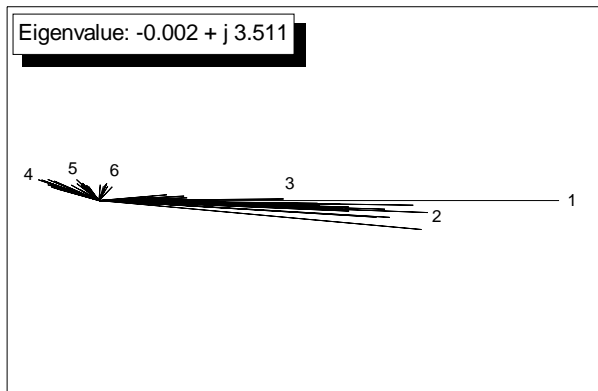
Figure 12. System Eigenvalues in the Absence of Damping Devices (362 State Variables)

Note in Figure 12 that eight eigenvalues have damping ratios below the minimum level of 5%. The objective of the study conducted in this section is to evaluate the capability of the methodology and software developed for locating and tuning various TCSC devices to simultaneously damp all the eight modes. The task of

controlling line power flows was not here assigned to these TCSC devices.

Adequate power oscillation damping is usually achieved in practice through power system stabilizers added to generating plants. When all the economically attractive damping sources are exhausted one should look for other options such as TCSC devices. However, for the purpose of methodology validation the damping of all the eight modes will be here exclusively effected through TCSC devices.

A major system mode is the South-Southeast interarea mode which is displayed, in a phasor diagram form, in Figure 13. Another critical one is the Itaipu multimachine mode (Figure 14), whose largest participation comes from the gigantic Itaipu power plant. The captions of these figures show the names of some generators which have high participation in the two mode shapes.



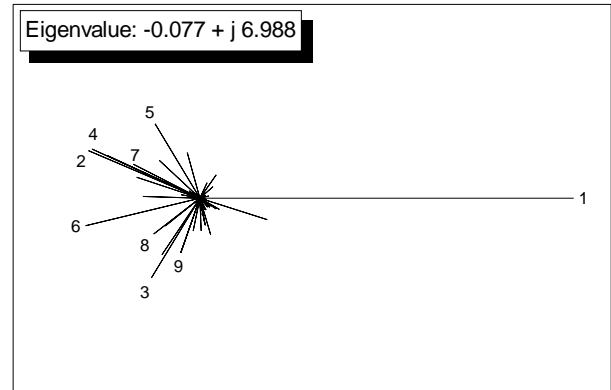
- | | |
|----------|---------------|
| 1-Jacuí | 4-C. Dourada |
| 2-Itaúba | 5-Promissão |
| 3-Itaipu | 6-Piratininga |

Figure 13. Rotor Speed Mode Shape of the South-Southeast Interarea Mode (0.56Hz)

A sequential strategy was adopted for locating and tuning the various TCSC damping devices. One mode was studied at a time, starting by selecting a set of the most adequate transmission lines in the system for placing the TCSC based on mode controllability or residue information.

The choice of the input variable to the TCSC damping device was based on mode observability factors [6] and frequency response analysis. This helped choosing variables which needed the least gain and phase compensation to damp the mode analyzed. In multivariable control terminology, the design procedure of this paper is *sequential loop closing* aided by an effective *loop-assignment* technique (see chapter 4 of [13]). The use of input variables from the

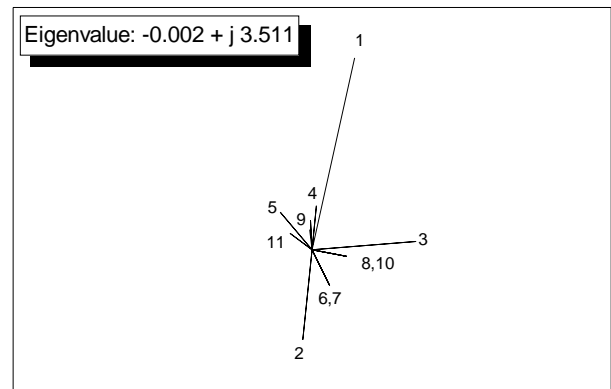
transmission network generally led to more complex compensation circuitry. Simpler and more robust designs were obtained by using rotor speed signals of selected machines as the TCSC inputs.



- | | | |
|------------------|---------------|------------------|
| 1-Itaipu | 4-Passo Fundo | 7-S. Osório (2M) |
| 2-S. Osório (4M) | 5-Itaúba | 8-S. Santiago 1 |
| 3-S. Cruz | 6-G.B. Munhoz | 9-S. Santiago 3 |

Figure 14. Rotor Speed Mode Shape of the Itaipu Multimachine Mode (1.11Hz)

The TCSC assigned to damp the South-Southeast mode was sited on the Assis-Maringá 230 kV line, which yielded the largest $\Delta P_{kj}(s)/\Delta B_{kj}(s)$ residue. This transmission line residue is numbered 1 in Figure 15, which depicts the major line residues in phasor diagram form. Note that, despite the large number of system lines (995) and the interarea nature of the mode, only eleven lines have residues of magnitude greater than 10% of the largest one. Six of these lines have their names given in the caption of Figure 15.



- | | |
|--------------------------|-------------------------------|
| 1-Assis - Maringá 230 | 4-Ivaiporã 765 - Ivaiporã 525 |
| 2-Areia - Ivaiporã 525 | 5-Itaúba 13.8 - Itaúba 230 |
| 3-Jacuí 13.8 - Jacuí 138 | 6-Gravataí 230 - Gravataí 500 |

Figure 15. Residues for the Transfer Functions

$$\Delta P_{kj}(\lambda_c)/\Delta B_{kj}(\lambda_c) \text{ for } \lambda_c = -0.002 \pm j3.511$$

The input signal to the TCSC located at the Assis-Maringá 230 kV line was chosen to be the

rotor speed of the 400 MVA Itaúba generator distant 700 kilometers to the South. This single TCSC effectively damped the South-Southeast mode. The TCSC designed to damp the Itaipu mode was placed at the Itaipu 765 kV transmission system and had the rotor speed of the Itaipu generator as the TCSC input.

Eight TCSC devices were sequentially located and tuned to bring all system modes to above a 5% damping level. The transfer functions for these eight TCSC damping devices comprised a washout and lead-lag blocks. TCSC controller parameters were determined from Nyquist plots of the appropriate $\Delta\omega_{gen}(s)/\Delta X_{ref}(s)$ transfer functions.

Compensation requirements for each one of the eight control loops were always below ± 20 degrees, calculated at the frequency of the oscillatory mode to be damped. The phase compensation needed for TCSC input signals were minimum for generator speeds and around 90 degrees for line powers (results not shown). These findings are in agreement with those reported in [1]. Figure 16 shows the loci of the system eigenvalues in the presence of the eight TCSC oscillation damping devices derived from generator speed.

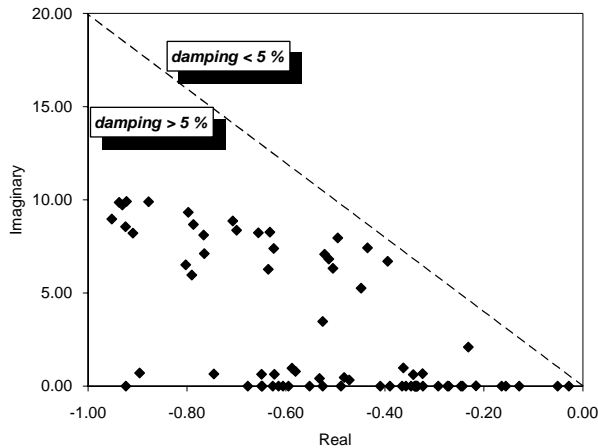


Figure 16. System Eigenvalues in the Presence of Eight TCSC Devices (375 State Variables)

Time response results are shown for a simultaneous disturbance to the mechanical power of three generators: $(0.01\Delta P_{Itaipu} - 0.01\Delta P_{Itaúba} + 0.005\Delta P_{Jupiá})$, where Itaipu, Itaúba and Jupia are large generating plants. This disturbance excites the major system modes. The variables pictured in the plots are the electrical power outputs of the same generators. The system step responses, in the absence and presence of the eight TCSC damping devices, are shown in figures 17 and 18 respectively.

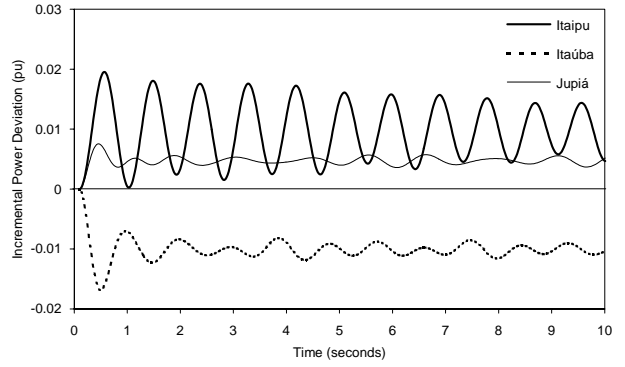


Figure 17. System without Damping Devices (362 States)

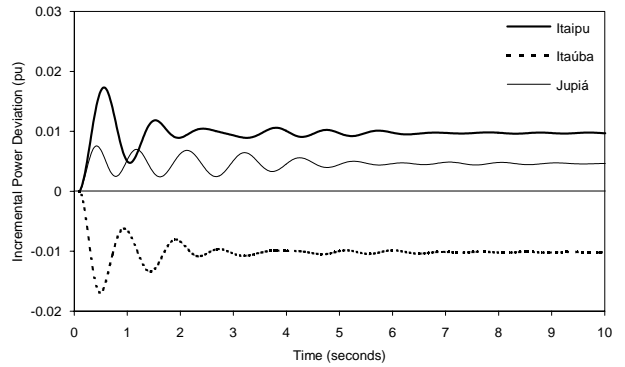


Figure 18. System with Eight TCSC Devices (375 States)

5. CONCLUSIONS

An efficient and mathematically rigorous algorithm for locating TCSC devices for damping oscillations in power systems is described. The results obtained for a large practical system validated the proposed methodology. The decentralized damping control of the multiple oscillatory modes was built by sequential single-loop designs, centering each loop in the damping of a specific mode. Detrimental dynamic interaction remained at a very low level by:

- proper choice of the locations and inputs to the TCSC devices;
- proper gain and phase compensation in the single loop designs based on frequency response plots of the large order system transfer functions.

The study will proceed by investigating the robustness of TCSC damping action to system changes [14]. The proposed algorithm can also yield TCSC siting information for SSR damping, if applied to the appropriate (R, L, C network transients represented) dynamic model of the power system [5].

TCSC damping concepts applied to multimachine oscillations were described in [15] for simplified system models. This paper further advances the work of [15] by providing TCSC siting and tuning methodologies suited for large practical power system models.

The "constant line power" strategy is meant to be applied to transmission systems having two or more parallel paths. The uncontrollable condition ($\lambda = 0$) observed in Case C eigensolution and time response results would occur in practice only during line outages. The system would remain, on the occurrence of a zero eigenvalue condition, drifting between the maximum and minimum output limits of the TCSC device. A protection scheme should, therefore, be devised to inhibit the TCSC "constant line power" control during some critical system contingencies. The TCSC damping function could however be left operational during such contingencies to enhance system performance.

The results of this paper are clear examples of the benefits gained from the complementary use of modal analysis, frequency response and step response tools which are presently available in modern small-signal stability packages. The control implementation of the TCSC "constant angle" strategy proposed in this paper is thought to be original.

6. ACKNOWLEDGMENT

The authors wish to thank Mr. Luiz Alberto S. Pilotto, from CEPEL, for the stimulating discussions on FACTS technology.

7. REFERENCES

- [1] **Proceedings: FACTS Conference 2**, EPRI publication **TR-101784**, Project 3022, December 1992.
- [2] **Technology and Benefits of Flexible AC Transmission Systems**, CIGRÉ Joint Session of Study Committees 14/37/38, Paris, August 30-September 5, 1992
- [3] **J. Urbanek, R. J. Piwko, E. Larsen and others**, "Thyristor Controlled Series Compensation Prototype Installation at the Slatt 500kV Substation", paper **92SM467-1 PWRD**, presented at the *IEEE/PES Summer Meeting*, Seattle, July 1992.
- [4] **N. G. Hingorani**, "Flexible AC Transmission", *IEEE Spectrum*, April 1993, pp 40-45.
- [5] **E. Larsen, C. Bowler, B. Damsky, S. Nilsson**, "Benefits of Thyristor Controlled Series Compensation", *International Conference on Large High Voltage Electric Systems (CIGRÉ)*, paper **14/37/38-04**, Paris, Sept. 1992.
- [6] **N. Martins & L. T. G. Lima**, "Determination of Suitable Locations for Power System Stabilizers and Static Var Compensators for Damping Electromechanical Oscillations in Large Scale Power Systems", *IEEE Transactions on Power Systems*, Vol. **PWRS-5**, pp. 1455-1469, November 1990.
- [7] **N. Martins & L. T. G. Lima**, "Eigenvalue and Frequency Domain Analysis of Small-Signal Electromechanical Stability Problems" *IEEE Symposium on Application of Eigenanalysis and Frequency Domain Methods for System Dynamic Performance*, publication **90TH0292-3PWR**, pp. 17-33, 1990.
- [8] **P. Kundur, G. J. Rogers, D. Y. Wong, L. Wang, M. G. Lauby**, "A Comprehensive Computer Program Package for Small Signal Stability Analysis of Power Systems", *IEEE Transactions on Power Systems*, **PWRS-5**, pp. 1076-1083, 1990.
- [9] **L. Wang, A. Semlyen**, "Application of Sparse Eigenvalue Techniques to the Small Signal Stability Analysis of Large Power Systems". *IEEE Transactions on Power Systems*, Vol. **PWRS-5**, pp. 635-642, 1990.
- [10] **V. Arcidiacono, E. Ferrari, R. Marconato, J. Dos Ghali, D. Grandez**, "Evaluation and Improvement of Electromechanical Oscillation Damping by Means of Eigenvalue-Eigenvector Analysis. Practical Results in the Central Peru Power System", *IEEE Transactions on Power Apparatus and Systems*, Vol. **PAS-99**, pp. 769-778, March/April 1980.

- [11] **F. L. Pagola, J. I. Pérez-Arriaga, G. C. Verghese**, "On Sensitivities, Residues and Participations. Applications to Oscillatory Stability Analysis and Control", *1988 IEEE Summer Meeting*, paper **88 SM 692-6**, 1988.
- [12] **N. Martins, N. J. P. Macedo, A. Bianco, H. J. C. P. Pinto, L. T. G. Lima**, "Proposal for a Benchmark System for Power System Oscillation Analysis and Control", invited paper presented at *CIGRÉ-Study Committee 38 International Colloquium on Power System Dynamic Performance*, Florianópolis, Brazil, Sept. 1993.
- [13] **J. M. Maciejowski**, "Multivariable Feedback Design", New York: Addison Wesley, 1989.
- [14] **J. F. Hauer**, "Reactive Power Control as a Means of Enhanced Interarea Damping in the Western U.S. Power System - A Frequency-Domain Perspective Considering Robustness Needs", in *IEEE Tutorial Course: Application of SVS for System Dynamic Performance*, publication **87 TH 01875 PWR**, pp. 79-82, 1987.
- [15] **F. P. de Mello**, "Exploratory Concepts on Control of Variable Series Compensation in Transmission Systems to Improve Damping of Intermachine/System Oscillations", *1993 IEEE Winter Meeting*, paper **93 WM 208-9**, 1993.

8. BIOGRAPHIES

Nelson Martins B.Sc. (72) Elec. Eng. from Univ. Brasilia, Brazil; M.Sc. (74) & Ph.D. (78) degrees from UMIST, UK. Dr. Martins works in CEPEL since 1978 in the development of computer tools for power system dynamics and control.

Hermínio J.C.P. Pinto B.Sc. (86) and M.Sc. (90) Elec. Eng. from Fed. Univ. of Rio de Janeiro, Brazil. Since 1986 he is with CEPEL and his current work and interests include power system operation and control and parallel processing.

André Bianco B.Sc. (90) Elec. Eng. from Univ. Gama Filho and is now working towards his M. Sc. degree in the Catholic Univ. of Rio de Janeiro. His main interests are voltage stability and power system dynamic analysis.

Nilo J.P. Macedo B.Sc. (79) Elec. Eng. from Catholic Univ. of Rio de Janeiro and M.Sc. (92) from Fed. Univ. of Rio de Janeiro. Mr. Macedo is a senior engineer at Furnas Centrais Elétricas, where he works in power system operations planning.

APPENDIX

Small Power System Data

Frequency: 60 Hz;

System and Generator Base: 1000 MVA.

Line Data for All Cases

Line		Circuit	Impedance (%)	
From	To		R	X
1	2		0.70	10.0
2	3	#1	6.40	90.0
2	3	#2	6.40	90.0

Bus Data for Cases A, B, C and D

Bus	V pu	θ degrees	Pgen MW	Qgen MVA _r
1	1.000	15.9	500.	34.0
2	0.994	13.0		
3	1.000	0.0	-490.2	104.2

Bus Data for Cases E and F

Bus	V pu	θ degrees	Pgen MW	Qgen MVA _r
1	1.000	32.8	1000.	218.7
2	0.976	27.0		
3	1.000	0.0	-959.1	357.6

Generator Data

H = 5.00	X'd = 0.30	T'do = 7.50
Xd = 1.00	X"d = 0.25	T"do = 0.09
Xq = 0.70	X"q = 0.25	T"qo = 0.20

Reactances given in per unit; time constants and inertia in seconds

The generator excitation control, for all cases, has the first order transfer function

$$AVR(s) = 75 / (1 + s 0.05)$$

The remaining system data is given along the section 3 of this paper.